Dynamic Light Scattering and Fluorescence Study of the Interaction between Double-Stranded DNA and Poly(amido amine) Dendrimers

ARTICLE *in* BIOMACROMOLECULES · JUNE 2007

Impact Factor: 5.75 · DOI: 10.1021/bm061194z · Source: PubMed

3 AUTHORS, INCLUDING:

Karin Schillén
Lund University
80 PUBLICATIONS **2,876** CITATIONS

SEE PROFILE

Interaction between DNA and Charged Colloids Could Be Hydrophobically Driven

Marité Cárdenas,*,† Karin Schillén,† Dmitri Pebalk,†,‡ Tommy Nylander,† and Björn Lindman‡

Physical Chemistry 1, Center for Chemistry and Chemical Engineering, Lund University, P.O. Box 124, SE-221 00 Lund, Sweden, and Polymer Division, Chemistry Department, Moscow State University, 119992 Leninskie Gory, Moscow, Russia

Received September 15, 2004; Revised Manuscript Received November 24, 2004

The interaction of DNA with amino-functionalized polystyrene particles has been studied by using a dynamic light scattering (DLS) technique. In 10 mM NaBr solution the particles have a hydrodynamic radius of 76 nm and the DNA macromolecule investigated (double stranded) has a hydrodynamic radius of 107 nm. At very low DNA concentrations, DNA adopts a flat conformation on the particle surface. If the DNA concentration is increased above 0.1 μg/mL, the thickness of the DNA layer increases, suggesting the presence of large loops and tails. Although the particles contain primary amino groups, they have a negative net charge under the conditions used in this work. Thus, the driving force for DNA adsorption is not of electrostatic origin but rather due to a hydrophobic effect. Addition of cationic surfactant to the DNA-precoated amino-functionalized particles induces changes in the adsorbed layer conformation, in agreement with the coadsorption of cationic surfactant.

Introduction

In the cell nucleus DNA is embedded in a complex matrix formed by, for example, lipids and proteins. This causes dramatic changes in the DNA macromolecule conformation in a way that makes it possible for this giant molecule to pack into highly confined spaces. The histones, which are small cationic proteins that form aggregates with a 10 nm diameter around which two turns of the DNA strand can be wrapped, are an important component in this matrix.[1] Mimicking this type of complexation process, DNA immobilized onto solid supports could be used as a tool in medical, pharmaceutical, and various diagnostic applications.[2] Additionally, DNA compacted by different cationic agents has been considered as a plausible vehicle for gene delivery.[3] Lately, studies of the interactions between DNA and charged colloids have been used as models for understanding the driving forces for DNA packing into cells and to investigate how this correlates with the way this macromolecule interacts with different particles in the cell.[4] However, most studies have so far been conducted with particles with a diameter larger than 200 nm, mainly using aminated latex particles.[5−7] Previously, we have shown that DNA also interacts with slightly anionic, hydrophobic latex particles with a diameter of 110 nm.[8] This was evident from the increase in the hydrodynamic radius observed from dynamic light scattering (DLS) measurements.[8] Moreover, the addition of a cationic surfactant to this DNA−particle system induced a dramatic decrease of the hydrodynamic radius of the particles, mainly due to the compaction of the DNA chains.[8] Recent SANS measurements on deuterated latex particles have also shown DNA layer compaction where large surfactant aggregates (much larger than single spherical micelles) are formed within the adsorbed layer.[9] In the present work, we have further investigated the nature of the DNA−particle interaction. For this purpose the effect of the charge of the particles on the interaction with DNA was studied by using amino-functionalized particles.

Experimental Section

Materials. Salmon sperm DNA was purchased from Gibco, BRL, and used as received. As stated by the manufacturer, this DNA is double-stranded, is 2000 ± 500 base pairs (bp) in length as determined by 1% TAE agarose gel analysis, and is free from Dnase and Rnase. The hydrodynamic radius (R_H) was determined at infinite dilution by dynamic light scattering (DLS) and found to be 107 ± 5 nm.[8] Cetyltrimethylammonium bromide (CTAB; Merck, pa quality) and sodium bromide (Aldrich, extra pure quality) were used as received. Polybead amino-functionalized polystyrene microspheres (2.61% solid latex in aqueous solution) were purchased from Polysciences Inc. and dialyzed against water and 10 mM NaBr solution prior to use. The electrophoretic mobility of the amino-functionalized particles in solution containing 10 mM NaBr (pH ∼6) was determined with a Zetasizer IV (Malvern Instruments). DNA, CTAB, and amino-functionalized polystyrene (aPS) particle stock solutions were prepared in 10 mM NaBr solution that was previously filtered through a sterile 0.20 μm Minisart filter (Sartorius, Germany). Water purified by a Milli-Q system (Millipore Corp., Bedford, MA) was used in all solutions. The DNA concentration in the stock solution was measured

* Corresponding author. E-mail address: marite.cardenas@fkem1.lu.se.
† Lund University.
‡ Moscow State University.

10.1021/bm049422h CCC: $30.25
Published on Web 01/15/2005

spectrophotometrically at 260 nm, using an extinction coefficient equal to 0.02 mL μg^{-1} cm^{-1} for ds-DNA. The ratio between the absorbance at 260 nm and at 280 nm was about 1.8−1.9 and the absorbance at 320 nm was negligible, which indicates that no protein contamination was present. The final solutions were prepared by diluting the appropriate amount of the stock solutions with 10 mM NaBr solution and letting them equilibrate for certain time.

Particle Characterization. The ζ-potential of the aPS particle solution in 10 mM NaBr (pH 6) was found to be -3.2 ± 0.2 mV. Although the surface of the particles is functionalized with primary amino groups, it also contains sulfate groups, as specified by the provider. Moreover, adsorption of bromide ions to the particle's surface is expected due to the large binding capacity of this ion.[10,11] Therefore, the particles should be regarded as zwitterionic with a zero net charge at around pH 2.9.[12] It is noteworthy that the bare aPS particle dispersion spontaneously aggregates within a time scale of 2 weeks after dialysis against 10 mM NaBr solution. Earlier it has been shown that the degree of protonation of the charge groups present on this type of particle in aqueous solution is strongly pH-dependent.[5,12] Zhao et al.[12] used amino-functionalized latex particles with characteristics similar to those used in this work (the method of preparation is based on emulsion polymerization, and the amino groups are added after the beads are made). They found that, within the pH 5−9 range, the particles have a constant negative electrophoretic mobility with an isoelectric point of 2.9. Consequently, the electrophoretic mobility becomes less negative for pH values below 5. Above pH 9, on the other hand, a more negative electrophoretic mobility than at pH 5−9 was found, indicating further ionization of the sulfate groups and deprotonation of the amino groups. This is a reflection of the different pK_a values for HSO_4^- (1.9) and $R-NH_3^+$ (~10). The hydrodynamic radius of the aPS particles at infinite dilution is found to be 76 ± 1 nm, which is larger than the specification of the manufacturer (50 ± 16 nm). This apparently large difference comes from the different sizing method used by the manufacturer (electron microscopy). Electron microscopy gives the number-average radius while DLS gives a *z*-average and also includes an aqueous hydration layer around the particle. Moreover, another contribution to the observed difference in radius could be due to different conformations that the particle might take in various aqueous environments. Zhao et al.[12] also found that the size of the particle changed depending on the solvent conditions (pH and salt content). This was related to the different types of conformations that the hairy interface of the latex particles could attain when subjected to different solvent qualities.

Dynamic Light Scattering. The setup utilized for the dynamic light scattering (DLS) measurements is an ALV/DLS/SLS-5000F, CGF-8F based compact goniometer system from ALV-GmbH. (Langen, Germany). The light source is a CW diode-pumped Nd:YAG solid-state Compass-DPSS laser with a symmetrizer from COHERENT, Inc. (Santa Clara, CA). It was operated at 532 nm with a fixed output power of 400 mW. The laser intensity could be modulated by an external compensated attenuator from Newport Corp. The instrumental settings have been described in detail previously.[13] In this work, the temperature was controlled at 25 °C ± 0.1 °C and the scattering angle (θ) was varied from $\theta = 50°$ to 135°. Two multiple τ digital correlators (with a total of 320 exponentially spaced channels) were utilized to produce the time correlation function of the scattered intensity with an initial real-time sampling time of 12.5 ns. The normalized intensity correlation function $g^{(2)}(t)$ is related to the normalized time correlation function of the electric field [$g^{(1)}(t)$], by Siegert's relation: $g^{(2)}(t) - 1 = \beta|g^{(1)}(t)|^2$, where t is the lag time and β (≤ 1) is a coherence factor that accounts for deviation from ideal correlation and the experimental geometry. For polydisperse particle sizes or for different modes of motion, $g^{(1)}(t)$ may be described by

$$g^{(1)}(t) = \int_0^\infty \tau A(\tau) \exp(-t/\tau)\, \mathrm{d} \ln \tau \qquad (1)$$

where τ is the relaxation time and $A(\tau)$ is the relaxation time distribution.

The experimental intensity correlation functions ($g^{(2)}(t) - 1$) were analyzed by regularized inverse Laplace transformation (RILT) to obtain the relaxation time distribution. The RILT analysis uses the calculation algorithm REPES,[14−16] incorporated in the GENDIST analysis package.[16,17] We display the DLS results as relaxation time distributions that are expressed as $\tau A(\tau)$ vs $\log(\tau/\mu s)$ and normalized with the maximum peak height. From the DLS data, the apparent size of the particles can be determined. In the limit of small scattering vectors, **q**, the apparent translational diffusion coefficient (D) at finite concentration can be calculated from the relaxation rate Γ, which is obtained from the first moment of the translational mode in the relaxation time distribution

$$D = \lim_{q \to 0}\left(\frac{\Gamma}{q^2}\right) \qquad (2)$$

where q is the magnitude of the scattering vector [$q = 4\pi n_0 \sin(\theta/2)/\lambda$, where n_0 is the refractive index of water, λ is the incident wavelength, and θ is the scattering angle] and $\Gamma = 1/\tau$. Here, D is obtained from the slope of Γ as a function of q^2, where Γ has been measured at different scattering angles.

The apparent hydrodynamic radius (R_H^{app}) is related to the diffusion coefficient at finite concentration through the Stokes−Einstein relationship

$$R_H^{app} = \frac{kT}{6\pi\eta_0 D} \qquad (3)$$

where k is Boltzmann's constant, T is the absolute temperature, and η_0 is the viscosity of water. The relative error for both diffusion coefficient and hydrodynamic radius is calculated to be <6%.

Results and Discussion

1. Interaction between DNA and the Latex Particles. Figure 1a presents a collection of representative relaxation time distributions obtained from the inverse Laplace transformation analysis of the corresponding intensity correlation

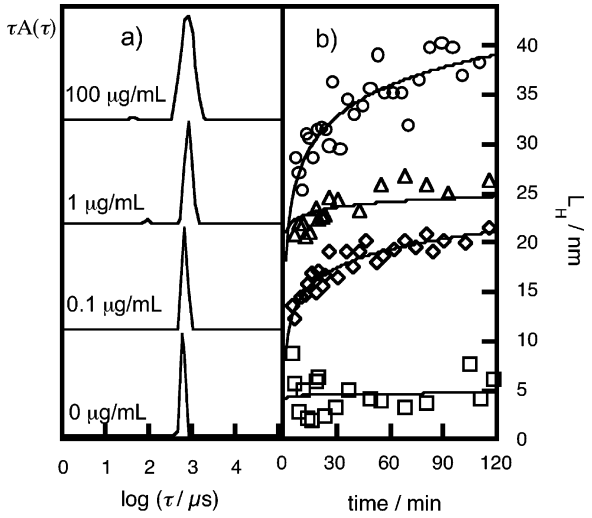

Figure 1. (a) Relaxation time distributions at $\theta = 90°$ for 0.0005 wt % amino-functionalized polystyrene particle solutions in 10 mM NaBr containing 0, 0.1, 1, and 100 μg/mL DNA measured after 48 h of equilibration. (b) Hydrodynamic layer thickness for DNA-coated amino-functionalized polystyrene particles as a function of elapsed time. The total DNA concentration is 0.1 μg/mL (squares), 1 μg/mL (diamonds), 10 μg/mL (triangles), and 100 μg/mL (circles). Lines are guides to the eye only.

functions from DLS measurements on solutions of 0.0005 v/v% aPS particles in 10 mM NaBr and with increasing concentrations of DNA. The correlation function of bare aPS particles is a single-exponential function, which corresponds to a narrow monomodal relaxation time distribution. This mode is attributed to the translational diffusion of the aPS particles. A diffusion coefficient is calculated from the linear q^2 dependence of the relaxation rate Γ of this mode (eq 2), and from this an apparent hydrodynamic radius (R_H^{app}) of 74 ± 1 nm is estimated using eq 3. This value should be compared to the value at infinite dilution (76 nm), which shows indirectly the positive concentration dependence of the translational diffusion coefficient. When DNA is added in increasing amount, the translational mode progressively shifts toward longer relaxation times, in accordance with a particle growth due to DNA adsorption. This occurs although the net charge of the bare aPS particle is negative (see Experimental Section), which indicates that the adsorption is driven by hydrophobic, nonelectrostatic interactions with the aPS surface. The driving force for the observed aPS−DNA interaction might then be the entropic gain when the water molecules in close vicinity to the hydrophobic surface are liberated from the surface into the bulk. Note that the hydrophobic tails present in the latex particles could interact with the DNA macromolecules, perhaps partially exposing the hydrophobic moieties hidden in the double helix, in a similar way to the tails of the nucleosome particles.[18]

To easily visualize the changes in hydrodynamic radius upon DNA addition to 0.0005 v/v% aPS dispersion, we define the hydrodynamic adsorbed layer thickness (L_H) as the difference between R_H^{app} of the coated and bare particles. Figure 1b gives the time dependence of L_H for different DNA concentrations in the aPS particle dispersion. Adsorption from a 0.1 μg/mL DNA solution gives rise to a small increase in R_H^{app} that corresponds to a L_H of only 4 nm. If the DNA concentration is further raised (>0.1 μg/mL), the increase in L_H at equilibrium is more pronounced. For instance, a 50% increase in particle size is found at the highest DNA concentration studied in this work. From easy geometrical calculations and the composition of the samples, we can estimate the number of DNA molecules per particle: there are about 10 DNA molecules per particle for solutions containing 0.1 μg/mL DNA. For the largest concentration used (100 μg/mL), the DNA-to-particle ratio rises to ~15 000. Although it is hard to imagine 15 000 DNA molecules attached to a single latex particle, we are not able to detect free DNA in solution in the DNA concentration regime studied. Indeed, previously free DNA was shown to coexist with DNA-coated latex particles at a total DNA concentration of 300 μg/mL (see ref 8 for details). An adsorption isotherm could not be measured, since the latex particles did not settle completely even after 1 h of centrifugation at 15 000 rpm.

We can now compare the approximate surface area of the bare particles [$A_{aPS} = 4\Pi(R_H^{app})^2$] with the area per DNA chain ($A_{DNA} = l_p d$, where the contour length is $l_p = 680$ nm and the diameter of the DNA double helix is $d = 2.2$ nm). For $R_H^{app} = 74$ nm, $A_{aPS} = 68\,800$ nm^2, while $A_{DNA} = 1500$ nm^2. Then, $A_{aPS}/A_{DNA} = 46$, implying that several DNA macromolecules can adsorb in a flat configuration on the surface of the bare particles. As the total DNA concentration is raised, the particles undergo a progressive increase in the hydrodynamic radius from 8% up to 50% larger than the size of the bare aPS particle. When the DNA concentration is increased above 0.1 μg/mL, a significantly thicker layer is formed on the particle, which can be interpreted as a layer that now consists of long loops and tails of the DNA chain extending toward the bulk solution. Indeed, increasing the DNA concentration above 0.1 μg/mL not only induces a shift and broadening of the translational mode but a new fast peak develops (see Figure 1a). This fast mode does not show any q^2 dependence through the origin; hence it does not correspond to translational motion and could be due to the internal motions within the tails and loops of the adsorbed chains. Earlier dynamic light scattering measurements on DNA macromolecules in aqueous solution have shown that both a slow translational mode and a fast internal motion mode that is coupled to the translational mode occur in the relaxation time distributions (see ref 8).[19,20] This internal mode was shown to disappear when the DNA molecule was compacted by cationic amphiphiles, indicating the formation of compact globular species.[8] As shown in Figure 1b, the change in R_H^{app} due to the adsorption of DNA from a solution free of surfactant quickly leveled off, reaching the steady-state value within the first 1.5 h. However, most of the adsorption seems to occur within the first 20−30 min. This is in agreement with an ellipsometry study on the adsorption of DNA to hydrophobized silica wafers in which the adsorption is very rapid during the first 15 min followed by a slow adsorption period.[21] It should be pointed out that the resulting DNA-coated amino-functionalized particles are indeed more stable than the bare ones. They remained stable for months in the dispersion, taken as a result of the increase in negative charge of the colloidal particle due to the interaction with DNA macromolecules.

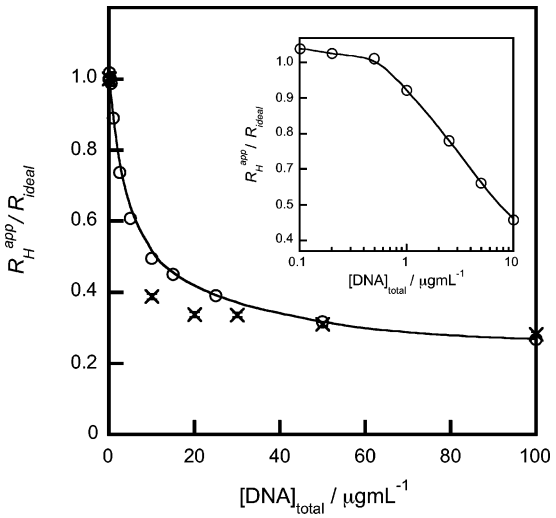

Figure 2. Ratio between the experimental radius and the calculated ideal one for DNA-coated particles versus the total DNA concentration in the solution for amino-functionalized (circles) and nonfunctionalized (crosses) polystyrene particles. The line is a guide to the eye only. Inset shows the low-concentration region.

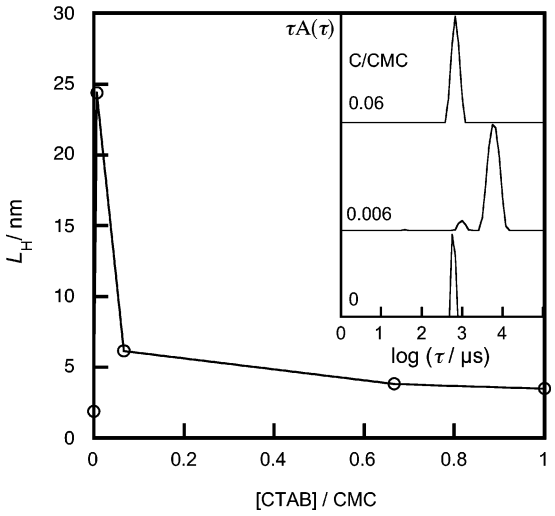

Figure 3. Hydrodynamic adsorbed layer thickness (L_H) for CTAB-coated amino-functionalized polystyrene particles as a function of CTAB concentration in 10 mM NaBr solution. Cmc denotes the critical micellar concentration (cmc = 0.15 mM for CTAB in 10 mM NaBr solution). The inset displays the relaxation time distributions at θ = 90° for 0.0005 v/v % amino-functionalized polystyrene particle solutions in 10 mM NaBr containing (from bottom) 0 μM (C/cmc = 0), 1 μM (C/cmc = 0.006), and 10 μM (C/cmc = 0.06) measured after 3 h of equilibration.

As a comparison, the ideal radius (R_{ideal}) for DNA-coated polystyrene particles can be calculated by simply considering a radius growth due the weight (and thereby volume) increase if we assume that all DNA present in solution adsorbs onto the particles (no steric or electrostatic considerations are involved). Figure 2 shows the ratio of the radius measured for DNA-coated amino-functionalized polystyrene particles and the ideal radius as a function of total DNA concentration. Below 1 μg/mL DNA, DNA adsorbs in an ideal manner, since the ratio is equal (or close) to unity. This is followed by a region with a linear deviation from ideality up to ~10 μg/mL DNA. Finally, a plateau value is reached at an experimental-to-ideal ratio of ~0.3. The same behavior is observed for the high DNA concentration data of the nonfunctionalized latex particle system from ref 8 (included in the figure). This is a clear indication that the relative adsorbed layer thickness is not changing with the nature of the particles surface, and therefore, hydrophobic interactions dominate over the electrostatic ones and constitute the driving force for DNA adsorption in the present system.

2. Interaction between a Cationic Surfactant and the Latex Particles. Since we want to study the effect of CTAB on the conformation of the adsorbed DNA layer on the particles, we first need to investigate the interactions between the cationic surfactant and the latex particles. Figure 3 shows the effect of CTAB addition to a latex particle dispersion in terms of the hydrodynamic adsorbed layer thickness defined in a way similar to that in Figure 1b. The inset gives a representative collection of relaxation time distributions for this system. As described in section 1, the DLS data for bare particles presents a narrow monomodal relaxation time distribution. Upon addition of very low CTAB concentration (C/cmc = 0.006, where the cmc is the critical micellar concentration of CTAB, here 0.15 mM), a large diffusive mode appears with a long relaxation time that is clearly resolved from the faster mode. The low amplitude mode is ascribed to the diffusion of single aPS particles with CTAB monomers adsorbed to their surfaces (L_H = 24 nm), whereas the slow diffusion mode corresponds to aggregates of several surfactant-coated aPS particles with a R_H^{app} > 500 nm. At this very low CTAB concentration the hydrophobic tails of the surfactant adsorbs onto the particles due to the hydrophobic effect; meanwhile, its cationic head electrostatically interacts with the sulfate groups and thus lowers the net charge of the particles, promoting faster particle aggregation. As the surfactant concentration is increased to C/cmc = 0.06, the relaxation time distribution becomes monomodal again with a corresponding L_H = 6 nm. A further increase in surfactant concentration to C/cmc = 0.6 causes a slight decrease in L_H to 4 nm. No change in L_H is observed if the CTAB concentration is further increased above the cmc of CTAB. The adsorption is expected to increase with the surfactant concentration, which in turn recharges the particles, as evidenced by the lack of particle aggregation. This is then correlated to the formation of surfactant aggregates (admicelles) onto the surface of the amino-functionalized polystyrene particles. Indeed, the layer thickness found for adsorbed CTAB micelles on flat silica, is around 3.5−4 nm.[22] These results confirm the negative net charge of the amino-functionalized polystyrene particles under the conditions used in the present work, which also was observed by Zhao et al.[23]

3. Interaction among DNA, a Cationic Surfactant, and the Latex Particles. To study the effect of a cationic surfactant on the conformation of the DNA layers adsorbed onto the amino-functionalized polystyrene particles, CTAB was added once steady-state was reached (after 2 days of mixing). Figure 4 gives the relaxation time distributions for DNA-coated aPSp (at two fixed DNA concentrations) in the presence of different amounts of CTAB, while Figure 5 presents the hydrodynamic adsorbed layer thickness for the DNA−CTAB-coated aPSp as a function of CTAB concentration. For particle solutions containing 0.1 μg/mL DNA,

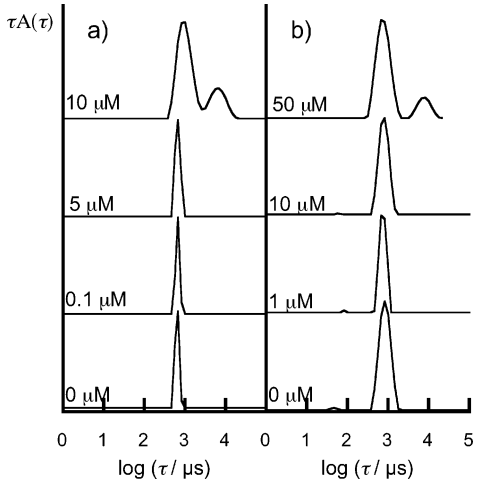

Figure 4. Relaxation time distributions at $\theta = 90°$ for 0.0005 v/v % DNA-precoated amino-functionalized polystyrene particle solutions containing in 10 mM NaBr with increasing CTAB concentrations. Fixed DNA concentrations of (a) 0.1 μg/mL and (b) 100 μg/mL were used.

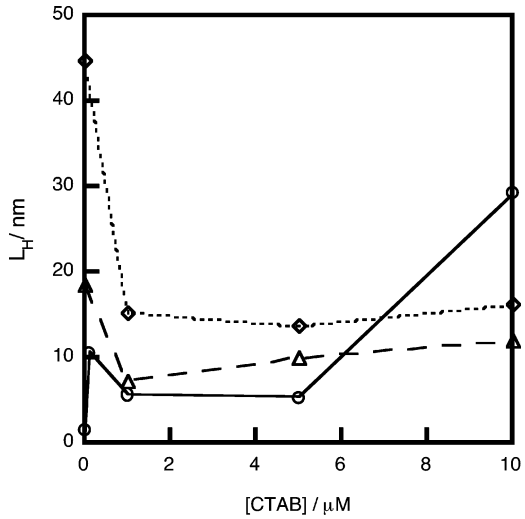

Figure 5. Hydrodynamic adsorbed layer thickness (L_H) for DNA-precoated amino-functionalized polystyrene particles as a function of increasing CTAB concentration in 10 mM NaBr solution. Fixed DNA concentrations of 0.1 μg/mL (circles), 1 μg/mL (triangles), and 100 μg/mL (diamonds) were used.

where DNA is adsorbed in a flat conformation (Figure 1b), addition of 0.1 μM CTAB (C/cmc = 0.0006) induces a slight shift of the translational relaxation mode toward longer relaxation times (Figure 4a). The results obtained from analysis of these data indicate that L_H increases to about 12 nm (Figure 5). CTA^+ ions coadsorbed onto the particle surface may thus induce further DNA adsorption from the bulk onto the particle surface as observed before by ellipsometry.[21] Further addition of CTAB causes a decrease in L_H to ~5 nm, which means that CTAB molecules slightly compact the adsorbed DNA layer at this stage. For 10 μM CTAB (C/cmc = 0.06), however, aggregation of the DNA−CTAB-coated particles occurs, as evidenced by the development of a slower mode that shows a q^2 dependence, i.e., a diffusive mode. If instead 100 μg/mL DNA was used, where DNA adsorbs in an extended conformation toward the bulk (Figure 1b), addition of CTAB shifts the translational mode of the particles toward shorter relaxation times

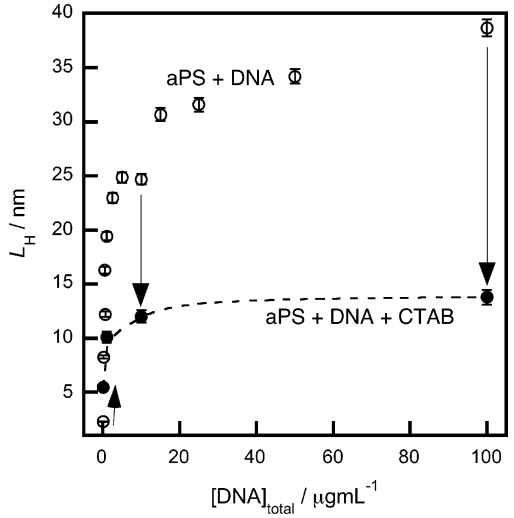

Figure 6. Hydrodynamic adsorbed layer thickness (L_H) as a function of total DNA concentration with (filled circles) and without (open circles) the presence of 1 μM CTAB. Error bars are included in the figure. Lines have been drawn as guides for the eye. Arrows point out changes in L_H upon CTAB addition.

(Figure 4b). For instance, L_H changes from 45 to 13−14 nm, regardless of the CTAB concentration within the range where no aggregation occurs. This decrease in hydrodynamic layer thickness is consistent with the collapse of the DNA chains due to the complexation with cationic amphiphile.[8,24,25] Finally, the slower mode indicative of particle aggregation appears at 50 μM CTAB. Particle aggregation occurs due to the neutralization of the DNA charges by the cationic surfactant, and therefore, more CTAB is required to aggregate the particles for higher DNA concentration.

In Figure 6 the adsorbed hydrodynamic layer thickness is presented as a function of the total DNA concentration in the particle solutions. As already discussed, the adsorbed layer conformation changes from essentially flat ($L_H \sim 2$ nm) into extended conformation with tails and loops (8 nm $< L_H <$ 38 nm, depending on the total DNA concentration) when increasing the DNA concentration above 0.1 μg/mL. Addition of the cationic surfactant CTAB to the DNA-coated aPSp under these conditions produces a compact layer. The degree of surfactant-induced DNA compaction, however, depends on the DNA concentration. The adsorbed DNA−CTAB layer thickness is ~5 nm for 0.1 μg/mL DNA, while it is >10 nm for higher DNA concentrations.

The layer of thickness of 5 nm observed at the lowest DNA concentration is reasonable if we take into account the molecular dimensions of the DNA strand (2 nm in diameter) and that of CTA^+ ions (a total length of 2.6 nm). Here one would expect that the mixed DNA−CTAB adsorbed layer might be composed of the DNA strand decorated with some sort of surfactant aggregates or distorted micelles. Although the net charge of the bare particles is negative, some electrostatic repulsion between the amino groups on the particle's surface and the surfactant headgroup is expected and might give rise to a more expanded layer (12 nm) at higher DNA concentrations. Another plausible explanation for the observed thicker adsorbed layer is the formation of multilayers. Is it noteworthy that the hydrodynamic layer

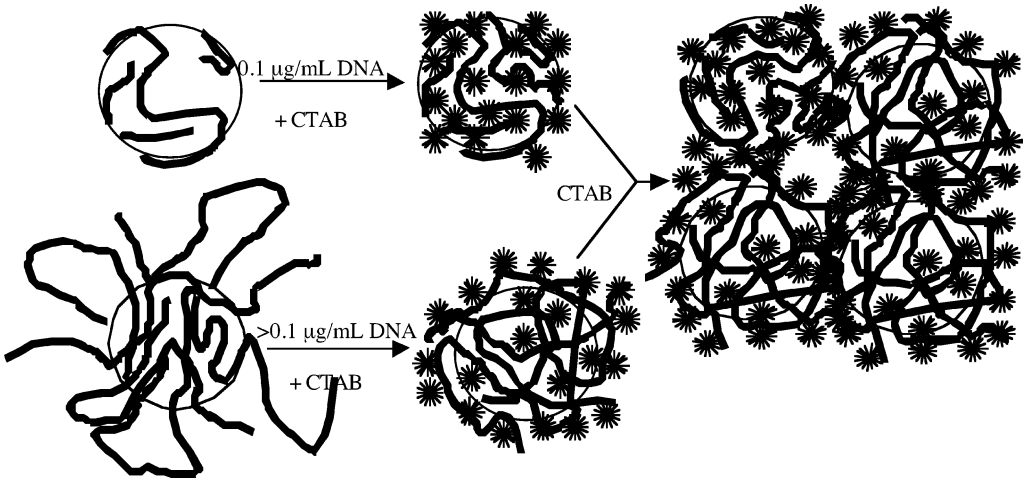

Figure 7. Schematic representation of the plausible structure of the DNA−CTAB-coated amino-functionalized polystyrene particles.

thickness of DNA−CTAB on latex particles that were not amino-functionalized was only 5−7 nm, regardless of the DNA concentration (1−600 μg/mL).[8] In that case, only negatively charged groups are present on the surface of the latex particles, and thus, no repulsive interaction is expected between the positively charged surfactant aggregates and the surface of the particle. As discussed above, the particles aggregate once a certain surfactant concentration is reached. This is represented schematically in Figure 7. Note that the cationic surfactants are depicted here as spherical micelles, since we cannot distinguish the structure of the surfactant aggregates within the mixed adsorbed layer. However, recent SANS data indicate that much larger surfactant aggregates are formed during the DNA compaction process.[9]

Detailed characterization of the nature of the surface of these latex particles in terms of charge density and hydrophobicity must be carried out before making any final conclusions about the forces that control the interactions between DNA and amino-functionalized polystyrene particles. On the basis of the results presented in this work, we conclude that DNA interacts with amino-functionalized particles even when they do not bear a positive net charge. In this case, the driving force for the adsorption arises from hydrophobic interactions and not from electrostatic effects. Specifically, the entropic gain of deconfining water molecules from the highly hydrophobic latex surface is the driving force behind DNA adsorption. Moreover, hydrophobic interactions between the polymeric tails of the latex particles and the hydrophobic moieties of the DNA macromolecule cannot be ruled out.

Acknowledgment. The authors acknowledge the Swedish Foundation for Strategic Research Program Colloid and Interface Technology and the Swedish Research Council for financial support.

References and Notes

(1) Stryer, L. *Biochemistry*, 4th ed.; Freeman, W. H. Co.: New York, 1995.
(2) Fodor, S. P. A. *Science* **1997**, *277*, 393.
(3) Verma, I. M.; Somia, N. *Nature* **1997**, *389*, 239.
(4) Kunze, K. K.; Netz, R. R. *Phys. Rev. Lett.* **2000**, *85*, 4389.
(5) Ganachaud, F.; Elaissari, A.; Pichot, C.; Laayoun, A.; Cros, P. *Langmuir* **1997**, *13*, 701.
(6) Gani, S. A.; Mukherjee, D. C.; Chattoraj, D. K. *Langmuir* **1999**, *15*, 7130.
(7) Elaîssari, A.; Chevalier, Y.; Ganachaud, F.; Delair, T.; Pichot, C. *Langmuir* **2000**, *16*, 1261.
(8) Cárdenas, M.; Schillén, K.; Nylander, T.; Jansson, J.; Lindman, B. *Phys. Chem. Chem. Phys.* **2004**, *6*, 1603.
(9) Cárdenas, M.; Dreiss, C.; Nylander, T.; Chan, C.; Cosgrove, T.; Lindman, B. *Langmuir* submitted for publication.
(10) Ninham, B. W.; Yaminsky, V. *Langmuir* **1997**, *13*, 2097.
(11) Cuccovia, I. M.; Agostinho-Neto, A.; Wendel, C. M. A.; Chaimovich, H.; Romsted, L. S. *Langmuir* **1997**, *13*, 5032.
(12) Zhao, J.; Brown, W. *J Colloid Interface Sci.* **1996**, *179*, 255.
(13) Jansson, J.; Schillén, K.; Olofsson, G.; Cardoso da Silva, R.; Loh, W. *J. Phys. Chem. B* **2004**, *108*, 82.
(14) Nicolai, T.; Brown, W.; Johnsen, R. M.; Stepanek, P. *Macromolecules* **1990**, *23*, 1165.
(15) Stepanek, P.; Brown, W. In *Dynamic Light Scattering*; Oxford University Press: New York, 1993; p 177.
(16) Johnsen, R. M.; Brown, W. In *Laser Light Scattering in Biochemistry*; Harding, S. E., Sattelle, D. B., Bloomfield, V. A., Eds.; 1992; p 449.
(17) Schillén, K.; Brown, W.; Johnsen, R. M. *Macromolecules* **1994**, *27*, 4825.
(18) Luger, K.; Mäder, A. W.; Richmond, R. K.; Sargent, D. F.; Richmond, T. J. *Nature* **1997**, *389*, 251.
(19) Sorlie, S. S.; Pecora, R. *Macromolecules* **1988**, *21*, 1437.
(20) Sorlie, S. S.; Pecora, R. *Macromolecules* **1990**, *23*, 487.
(21) Cárdenas, M.; Braem, A.; Nylander, T.; Lindman, B. *Langmuir* **2003**, *19*, 7712.
(22) Velegol, S. B.; B. D. F., Biggs, S.; Wanless, E. J.; Tilton, R. D. *Langmuir* **2000**, *16*, 2548.
(23) Zhao, J.; Brown, W. *Langmuir* **1996**, *12*, 1141.
(24) Mel'nikov, S. M.; Sergevej, V. G.; Yoshikawa, K. *J. Am. Chem. Soc.* **1995**, *117*, 2401.
(25) Lindman, B.; Mel'nikov, S.; Mel'nikova, Y.; Nylander, T.; Eskilsson, K.; Miguel, M.; Dias, R.; Leal, C. *Prog. Colloid Polym. Sci.* **2002**, *120*, 52.

BM049422H